A Simple Model for 100K-Year Oscillations in Glaciation

RICHARD S. LINDZEN

Department of Earth, Atmospheric, and Planetary Sciences, Massachusetts Institute of Technology, Cambridge, MA 02139

(Manuscript received 7 May 1985, in final form 2 December 1985)

ABSTRACT

A simple model is presented where response to forcing with components at 20K, 40K and 100K yr (where forcing, however, is strongly dominated by 20K yr) is primarily at 100K yr. The main features of the model are a very sensitive response of the snow and sea ice line to solar input, a threshold to transitions between large snow and sea ice coverage (to 53° latitude) and very little snow and sea ice coverage, and a glaciation cycle forced by the snow and sea-ice line position.

1. Introduction

The "100 000 year" climate cycle of the last 700 000 years has been so thoroughly discussed in the literature, that there is little point in repeating the discussion here (see Imbrie and Imbrie, 1979). Figure 1 shows a time series for $\delta\ ^{18}O$ variations, obtained from five deep sediment cores (Imbrie et al., 1984). The common interpretation is that the fluctuations are due to variations in glaciation. Although the periodicity is predominantly at 100K, other frequencies are clearly present. This is demonstrated in Fig. 2, which shows a power spectrum based on a 500K time series (Mason, 1976). Discernible but smaller peaks near 40K and 20K are present. Moreover, Fig. 1 suggests significant irregularity prior to 500K BP (before present).

Croll (1875) and (more thoroughly) Milankovitch (1930) argued that these glaciation fluctuations were forced by orbital variations and the associated changes in insolation. The orbital fluctuations consist mainly of three components (Berger, 1978):

1) precession of the position of the earth on its orbit at equinox (essentially the precession of the axis of rotation) with periods of 19K and 23K;
2) obliquity variations (i.e., changes in the tilt of the rotation axis) with a period of 41K; and
3) changes in eccentricity with a period of 100K.

For simple climate models, it is difficult to translate the above into forcing; however, there is little question, for example, that item 1 is much larger than item 3. This leads to the most obvious problem: namely, why the response to item 3 is so much greater than the response to item 1. Another less obvious problem is that, averaged over the globe, the insolation changes due to all of the orbital factors amount to no more than a few tenths of a percent of the solar constant (Suarez and Held, 1979). The ice ages seem a rather large response to such small forcing. Despite this, paleoclimatologists have recently argued strongly in favor of the Milankovitch hypothesis, having shown excellent phase coherence between glaciation variations and orbital variations (viz. Imbrie et al., 1984).

The usual approach, following Milankovitch (1930) has been to argue that insolation fluctuations at high latitudes in summer are of primary importance for glaciation. Presumably, such fluctuations determine whether snow deposited in winter melts or not in the summer. In the latter case accumulation will occur. Orbital variations do provide substantial fluctuations of this type. Indeed the obliquity variations (item 2), which when averaged over the year go to zero, become very important in this scenario. This scenario too has difficulties. As noted by Broecker (1984) the preceding scenario would lead to glaciation in the Northern Hemisphere out of phase with glaciation in the Southern Hemisphere. On the contrary, glaciation occurred essentially simultaneously in both hemispheres. A numerical simulation of this scenario (Suarez and Held, 1979), moreover, was dominated by a 40K-year periodicity with almost no 100K component.

A final feature of interest has emerged from the recent observation of Berner et al. (1979) that atmospheric CO_2 varied with glaciation from about 300 ppm during interglacials to 200 ppm during glacials. According to Lindzen et al. (1981) the radiative effect of such changes is comparable to variations in the solar constant of a few tenths of a percent, i.e., of the same order as the changes associated with orbital variations. The origin of the CO_2 fluctuations has been actively studied (Knox and McElroy, 1984). Observationally, the CO_2 effect represents a positive feedback so that it does not directly account for climate oscillations—in

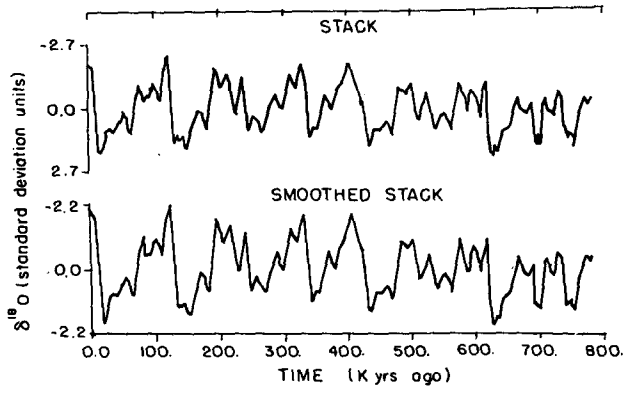

FIG. 1. Variations of $\delta\ ^{18}O$ vs time. The upper curve is an average over five deep-sea cores. The lower curve is a smoothed version of the upper curve. From Imbrie et al., 1985.

particular, for the dominance of the 100K period. A somewhat more subtle role will be discussed in section 2. The CO_2 effect does appear capable of contributing to the simultaneity of glaciation in Northern and Southern hemispheres, since CO_2 anomalies are rapidly transported.

The primary purpose of the present paper is to describe a simple and physically plausible climate model that produces glaciation cycles of primarily 100K periods in response to forcing that is dominated by 20K periods. The model itself, as well as a numerical example, will be given in section 2. The salient features of the model are concisely summarized in section 3, where we also examine the robustness of the results in section 2. Section 4 briefly presents some critical remarks.

Before proceeding, however, it may be worth remarking on an alternative approach to the problem of 100K-year climate oscillations—an approach that has been fairly popular in recent years. It is common when confronted by a large response to small forcing to seek resonances that, in turn, call for systems that freely oscillate near the desired period. Within the atmosphere–ocean system alone free oscillations of such long period are virtually impossible. However, a number of recent papers (Ghil and Le Treut, 1981; Peltier and Hyde, 1984; Saltzman et al., 1984, among others) have developed glacier models that can be tuned to oscillate at appropriate frequencies. At present, these models depend on posited feedbacks (between precipitation and glaciation, for example) which seem questionable at best. However, the possibility of such resonance remains. Suffice to say, no such possibility of free oscillation exists in the present model. Indeed, the only glacial physics included in the present model is that glaciers tend to grow or decay in response to whether the climate is cold or warm and that the relaxation time for glacial response is O(17K years). Some limitations of such a naive approach are discussed in section 2.

2. The model

It should be stated at the outset that we are not proposing a deductive theory of the 100K-year cycle. We question whether this is even possible at this stage. What we are presenting instead is a physically based simple model for climate and glaciation that has the property of responding to forcing strongly dominated by 20K periodicity with a glaciation cycle strongly dominated by a 100K period. The model also offers some insights into why intervals dominated by the 100K cycle are rare.

We begin with an energy balance model along the lines developed in Lindzen and Farrell (1977, 1980). The physics of these types of models is discussed in detail in these papers. In this paper we will confine ourselves to so-called annually averaged models. Such models are, in reality, not annually averaged; rather, they are *seasonless* models subject to annually averaged insolation. The fact that seasonally dependent features of the Milankovitch mechanism are not observed (Broecker, 1984) offers some hope that a seasonless model may be adequte, but problems of interpretation remain. We return to this point briefly in this section.

We next assume the Milankovitch hypothesis to be correct. As noted by Lindzen and Farrell (1977), the

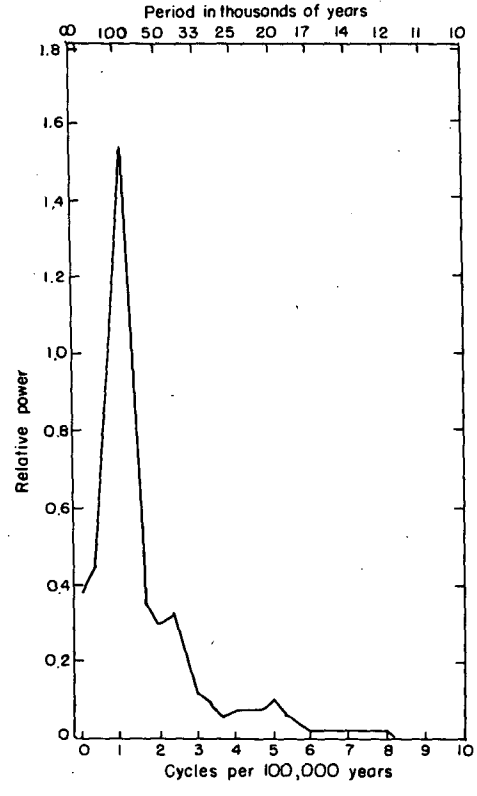

FIG. 2. Power spectrum of a time series of observed $\delta\ ^{18}O$ over the last 600K years. From Mason, 1976.

earliest models by Budyko (1960) and Sellers (1969) were inconsistent with this hypothesis because the changes in insolation required to significantly shift the ice/snow boundary were much greater than is provided by orbital variations. The traditional curve of x_s ($x_s = \sin\theta_s$, where θ_s is the latitude of the ice/snow boundary) versus Q (the insolation) is shown in Fig. 3. Also shown in Fig. 3 is Lindzen and Farrell's hypothesized curve, which would be consistent with the Milankovitch mechanism. Lindzen and Farrell (1980) were subsequently able to show that an energy balance climate model where simple diffusive or linear heat transport was replaced by baroclinic adjustment and where static stability was increased over ice/snow surface (as found by Held, 1976) would, in fact, yield an x_s versus Q curve like that needed for the Milankovitch mechanism to work. This curve is shown in Fig. 4. Note that for $Q/Q_0 = 1$, the least positive perturbation will move the ice/snow boundary to the pole while the least negative perturbation will move it to 53°. Moreover, larger positive perturbations will, obviously, not move the boundary beyond the pole, while larger negative perturbations will not move θ_s much below 53° because of the increase in climate stability for $\theta_s < 53°$. Figure 4 is simply meant to show that the stability curve *required* by the Milankovitch is physically achievable. Regardless, however, of the correctness of baroclinic adjustment, such a curve is required if we accept the Milankovitch hypothesis. Without any loss of generality we can replace x_s with a variable, S, having the value -1 for $x_s = 1$ and $+1$ for $x_s = 0.80$ ($\theta_s = 53°$). The sensitivity of x_s to small fluctuations is indicated by the substantial interannual variability of this quantity. However, the present work ignores such short period fluctuations. In the present model, with values of Q/Q_0 near one, S will, in fact, always reside near either $S = +1$ or $S = -1$.[1]

The next feature of our model concerns the transitions between $S = +1$ and $S = -1$. If we ignore the small unstable region near the pole, then it would appear that any small perturbation in Q will move S between $+1$ and -1. However, in the presence of the instability at $S = -1$, Q will have to overcome a threshold before S goes to $+1$. This instability (known as the "small ice cap" instability) originates in the difference between the snow/ice boundary being at the pole and there being no snow/ice at all. A discussion of this instability in the presence of diffusive heat transfer was given by Lindzen and Farrell (1977) and Lindzen and Farrell (1980) found it to also occur for baroclinic adjustment. It has been noted by Held and Suarez (1974) that the instability does not exist for all models of heat

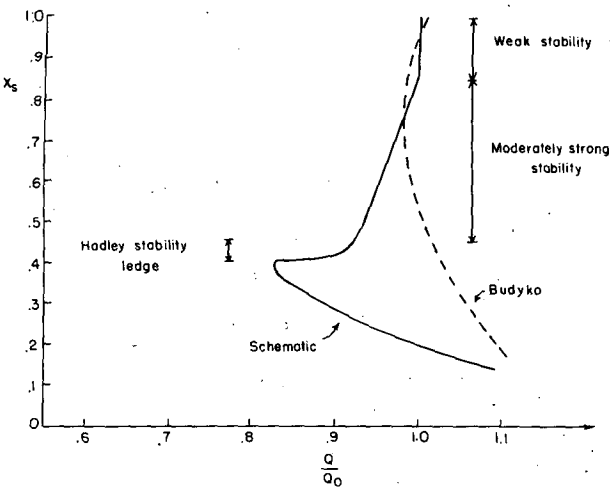

FIG. 3. The position of the ice/snow line vs solar constant. Shown are Budyko's (1969) curve and an idealized curve from Lindzen and Farrell (1977).

transport. However, North (1984) has recently argued for the reality of this feature. In addition to the "small ice cap" instability, CO_2 may provide a threshold mechanism as well. From the observations of Berner et al. (1979) and the theoretical models of Knox and McElroy (1984), it seems conceivable that $S = -1$ will lead to an increase in CO_2 which is equivalent in its effect to an increase in Q. Thus, to move to $S = +1$ will require Q/Q_0 to fall beneath a finite threshold. Similarly, if $S = +1$ we may expect a decrease in CO_2 equivalent to a decrease in Q, and to move to $S = -1$ will require Q to move above some finite threshold. The effect of these thresholds is schematically illustrated in Fig. 4. Our model assumes the existence of some such threshold mechanism. Let us pause to review our model to this point. Let

$$Q/Q_0 - 1 = f(t). \tag{1}$$

The response of S to (1) will depend on the initial value of S. If $S = -1$ initially, then S will change to $S = +1$ when $f(t) < f_1$ and S will change back to $S = -1$ when $f(t) > f_2 > f_1$. To make matters more concrete, let

$$f(t) = \epsilon\left(a_2 \sin\frac{2\pi t}{100\text{K}} + a_5 \sin\frac{2\pi t}{40\text{K}} + a_{10} \sin\frac{2\pi t}{20\text{K}}\right),$$
$$= \epsilon g(t), \tag{2}$$

where ϵ is some small number that we are unable to estimate at this point, but which represents the translation of the orbital forcing discussed in section 1 into a perturbation of Q/Q_0. For simplicity, we have approximated the period of the first orbital effect by 20K, and the second effect by 40K. This leads to $g(t)$ being periodic with a period of 200K. To simulate the dom-

[1] Of course, in a seasonal model, $S = +1$ will be associated with some finite ice/snow in winter, while $S = -1$ will be associated with some ice/snow retreat in summer.

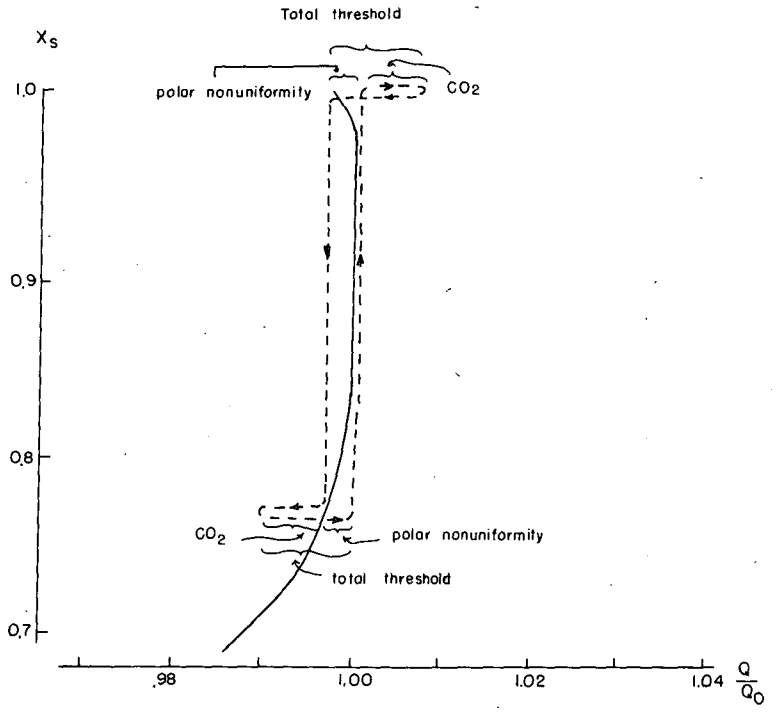

FIG. 4. The position of the ice/snow line vs solar constant as calculated by Lindzen and Farrell (1980). Also shown are the paths for climate transitions between $x_s = 1$ and $x_s = 0.8$, including threshold effects associated with both polar nonuniformity and CO_2 effects. See text for details.

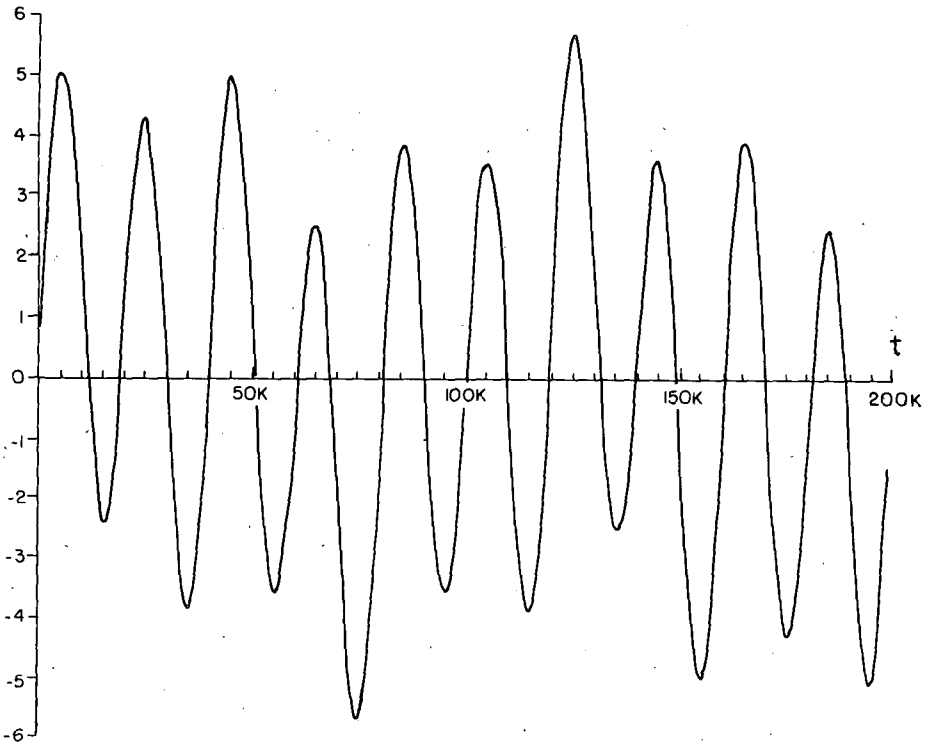

FIG. 5. Arbitrarily scaled model of the variations in solar heating associated with orbital variations.

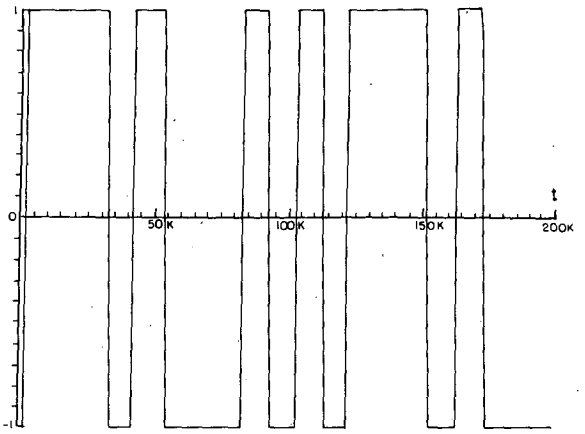

FIG. 6. Model variations of the ice/snow line associated with the variations of heating given in Fig. 5.

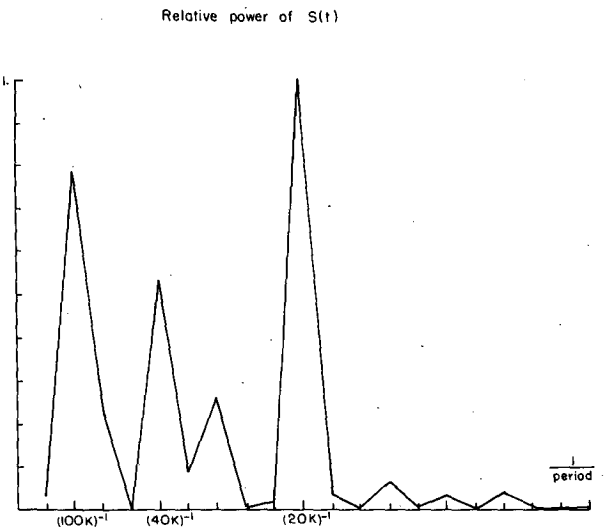

FIG. 7. Normalized power spectrum of the ice/snow variations in Fig. 6.

inance of the first orbital effect, let us take $a_2 = 1$, $a_5 = 1$ and $a_{10} = 4$; $g(t)$ is shown in Fig. 5. Next let us (by way of example) choose as our thresholds $f_1/\epsilon = -3$, and $f_2/\epsilon = +3$, and take $S(0) = -1$. The resulting $S(t)$ is shown in Fig. 6. It is quite clear that $S(t)$ displays more long period variability than does $g(t)$. This is made clearer by Fourier decomposing $S(t)$:

$$S(t) = \sum_{n=0}^{\infty} S_n \sin\left(\frac{2\pi nt}{200\text{K}} + \varphi_n\right). \tag{3}$$

Table 1 gives S_n and φ_n; Fig. 7 shows the normalized power spectrum for $S(t)$. While 20K supplies 16 times more power to $g(t)$ than does 100K, their contributions to $S(t)$ are almost equal. From Table 1 we also see that the threshold operator introduces phase lags relative to $g(t)$. In section 3 we will discuss the effects of different thresholds and of asymmetric thresholds. For the moment we will simply note that symmetric thresholds between ± 2.49 and ± 3.69 give identical values of $S(t)$; i.e., the results described are quite robust. Behavior for other thresholds and for asymmetric thresholds is given in section 3.

Of course, $S(t)$ in Fig. 6 does not look like Fig. 1. It is important, at this point, to recognize the sometimes ignored fact that $x_s(t)$ [or $S(t)$] does not refer to glaciation; rather it refers to fast-responding surface features like snow cover and sea ice, which increase albedo. A glacier with a wet surface has an albedo characteristic of water for example. The connection between glaciation and $S(t)$ leads to the last feature of our model: namely, although $S(t)$ does not describe the extent of glaciation, it almost certainly is what forces glaciation. Thus, if we let G = glaciation, we may write

$$\frac{dG}{dt} = S - aG. \tag{4}$$[2]

According to Imbrie and Imbrie (1980), $a = 1/17\text{K}$ while Weertman (1964) suggests $a = 1/(12\text{K} - 20\text{K})$, consistent with Imbrie and Imbrie whose value we will adopt. Equation (4) is trivially solved for G in terms of S:

$$G = G(0) + e^{-at}\int_0^t e^{at'}S(t')dt' \tag{5}$$

where $G(0)$ is chosen to yield 200K periodicity in G. If one did not so choose $G(0)$, the model would eventually still settle into such a periodicity. Figure 8 shows $G(t)$ corresponding to the $S(t)$ shown in Fig. 6. Clearly the response of G to S is roughly inversely proportional to frequency, and therefore further emphasizes longer periods (100K vs 20K). Indeed $G(t)$ bears a remarkable qualitative resemblance to Fig. 1. The primary difference is that Fig. 1 tends to show more rapid deglaciation phases than are seen in Fig. 8. This is almost certainly associated with the absence in our model of explicit glacial physics. Pollard (1983) argues that the rapid re-

TABLE 1. The amplitude and phase of $S(t)$ at the forcing frequencies.

Frequency (1/100K)	Amplitude	Phase* (deg)
2	0.67	−8
5	0.55	−16
10	0.75	−40

* Relative to forcing.

[2] Since (4) is linear, the sealing of G is irrelevant for our purposes.

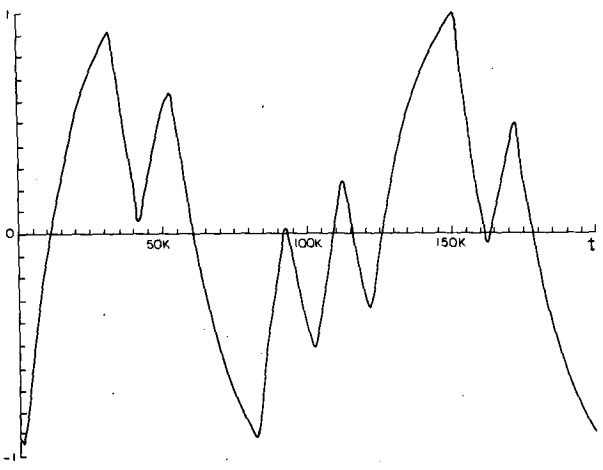

FIG. 8. Normalized variation of glaciation, $G(t)$, produced by model.

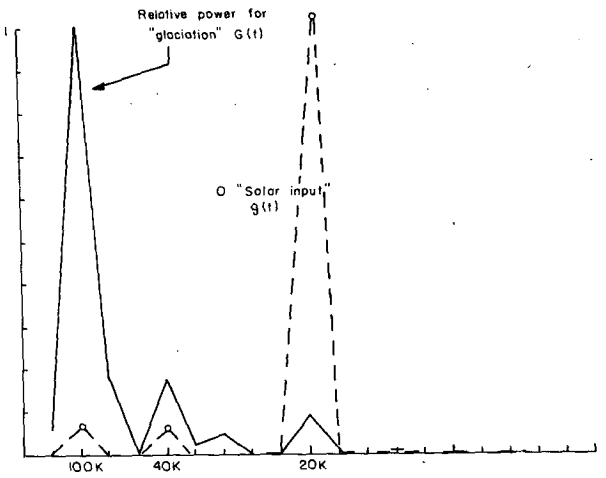

FIG. 9. Normalized power spectrum of the glaciation shown in Fig. 8. Also shown is the normalized power spectrum of the model solar heating variation shown in Fig. 5.

treat is associated with calving. Such features do not appear to be crucial to the overall picture presented in this paper.

Table 2 gives the Fourier coefficients of $G(t)$ while Fig. 9 shows its power spectrum as well as that of $g(t)$. For $G(t)$, 100K is about as dominant as 20K is for $g(t)$. More to the point, Fig. 9 closely resembles Fig. 2.

One additional matter deserves mention. Imbrie et al. (1984) found that glaciation at a given frequency lagged behind orbital fluctuations at the same frequency. Moreover, the lag at 20K was about 75° greater than the lag at 100K. This difference is about 3 times greater than the relaxation coefficient in Eq. (4) would suggest. However, the results in Table 2 are in good agreement with the observations because of the additional phase lag introduced by the threshold operator. To be sure, only relative, and not absolute phases are in agreement, but as Saltzman et al. (1984) point out, there is some plausible uncertainty in absolute phase.

3. Further analysis

In section 2 a climate model with the following crucial features was introduced.

TABLE 2. The amplitude and phase of $G(t)$ (normalized) at the forcing frequencies.

Frequency (1/200K)	Amplitude	Phase* (deg)
2	0.59	−55
5	0.25	−85
10	0.18	−120

* Relative to forcing.

1a) The ice/snow line could be anyplace between the pole and 53° for a constant $Q = Q_0$ (one might refer to this as a regionally neutral climate).

1b) It follows from 1a that if $Q = Q_0$, any perturbation above or below Q_0 will drive the ice/snow line to the pole or to 53°, respectively.

2) Once the ice/snow line is at the pole (at 53°), it becomes necessary for Q to fall below (rise above) Q_0 by a certain threshold in order for the ice/snow line to move to 53° (the pole).

3) The position of the ice/snow line is the forcing for glaciation.

Within the context of the above model, the crucial parameter determining whether one has a Milankovitch cycle or not is whether Q is sufficiently close to Q_0. As noted in Lindzen and Farrell (1977), Q can be viewed as not merely a measure of the solar constant but as a general descriptor of the radiative budget; changes in infrared properties and albedo can also generally be interpreted in terms of changes in Q. We shall expand on the meaning of "sufficiently close" shortly, but briefly we mean close compared to the variation in Q produced by orbital changes. Paleoclimatological data indicates that this condition, in fact, has rarely been met in the history of the earth.

In section 2, we showed that for a particular choice of forcing (i.e., a particular set of relative forcing amplitudes at 20K, 40K and 100K periods), a particular choice of threshold led to a response in glaciation which was strongly dominated by the 100K period even though the forcing was comparably dominated by the 20K period. In this section we will investigate the sensitivity of the preceding result to the choice of threshold for $a_2 = 1$, $a_5 = 1$ and $a_{10} = 4$ in Eq. (2). Other choices of a_2, a_5 and a_{10} lead to qualitatively similar results.

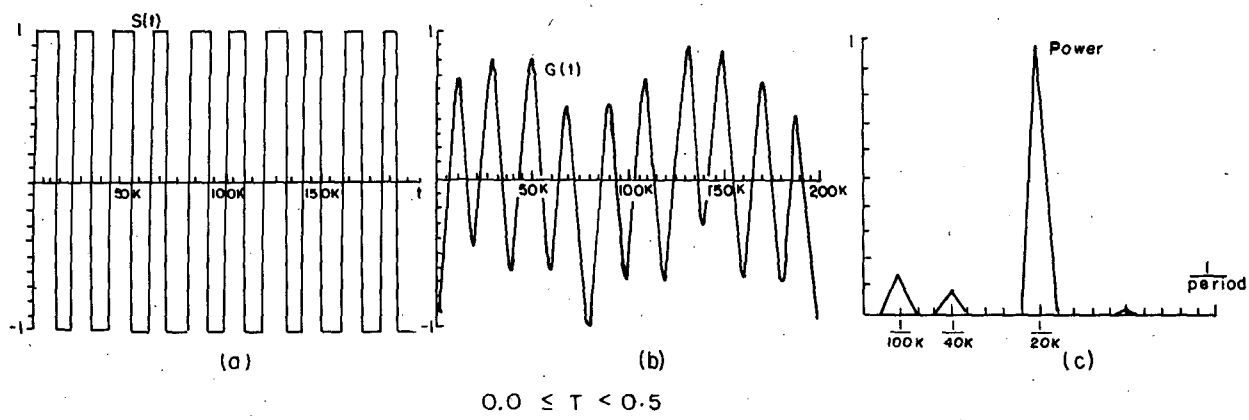

FIG. 10. Model response to the forcing in Fig. 5, but for a threshold, $T = 0$. (a) Variations of the snow/ice line, $S(t)$; (b) normalized glaciation, $G(t)$; (c) normalized power spectrum of the glaciation.

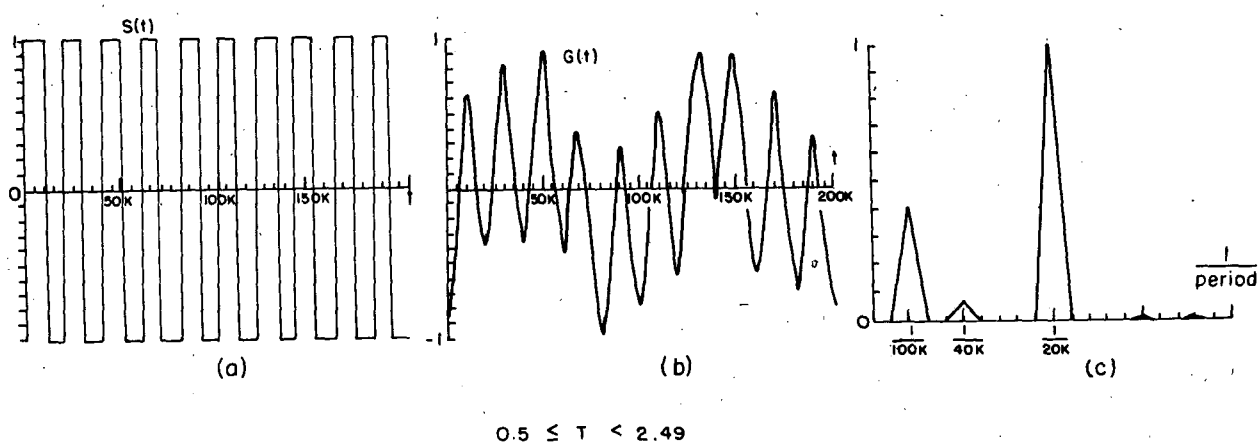

FIG. 11. As in Fig. 10 but for a threshold $T = 0.5$.

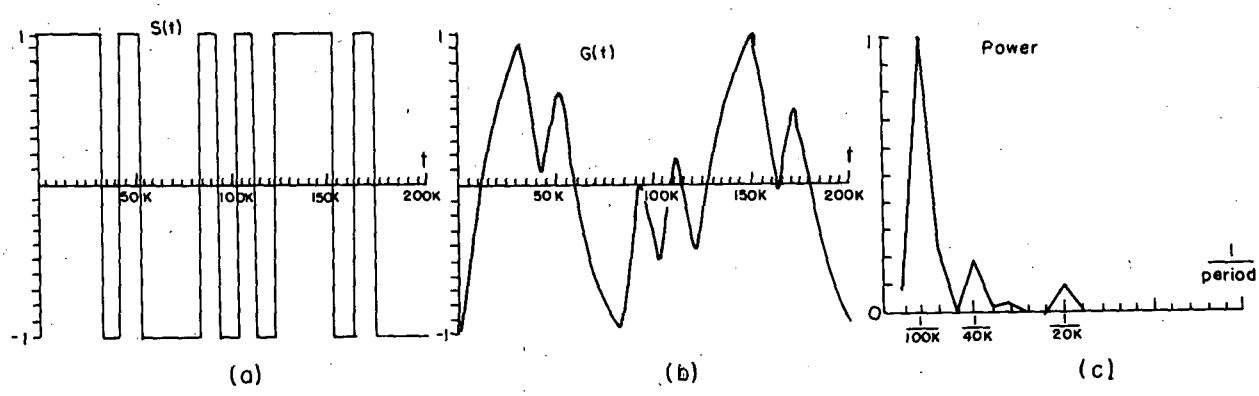

FIG. 12. As in Fig. 10 but for a threshold $T = 2.49$.

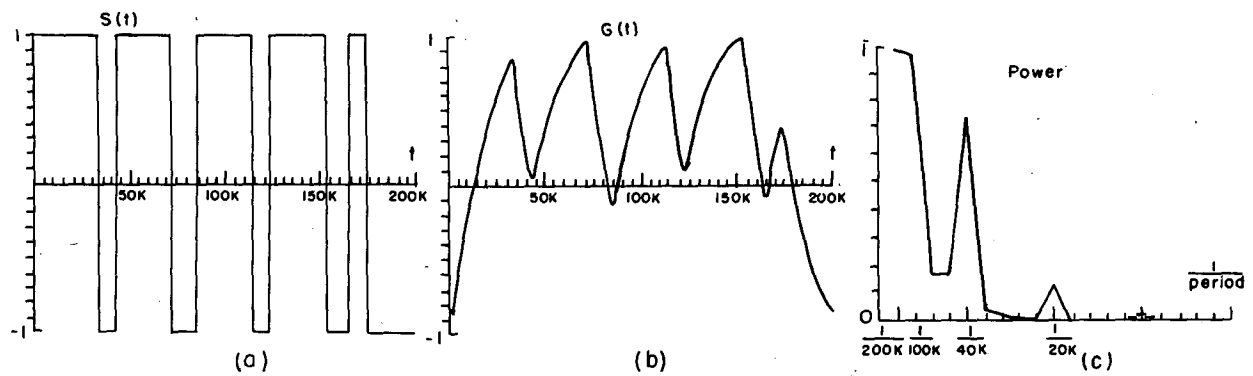

FIG. 13. As in Fig. 10 but for a threshold $T = 3.7$.

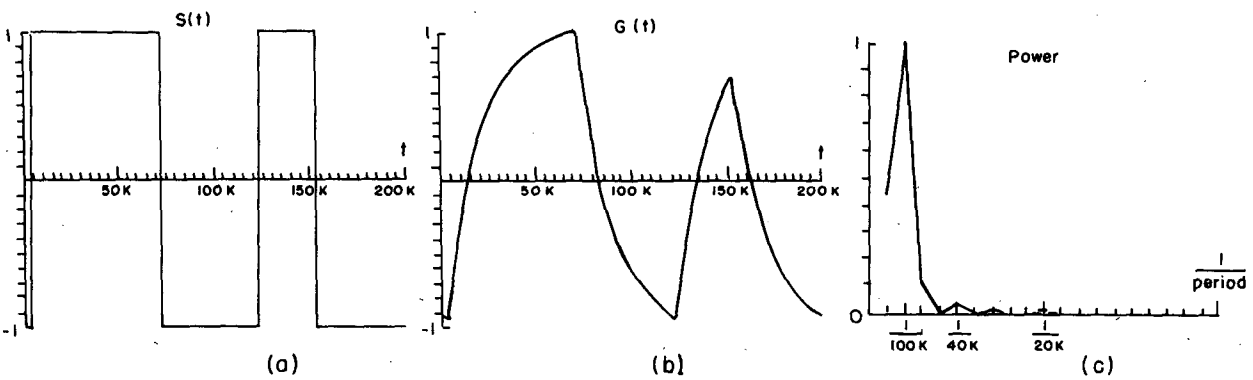

FIG. 14. As in Fig. 10 but for a threshold $T = 3.9$.

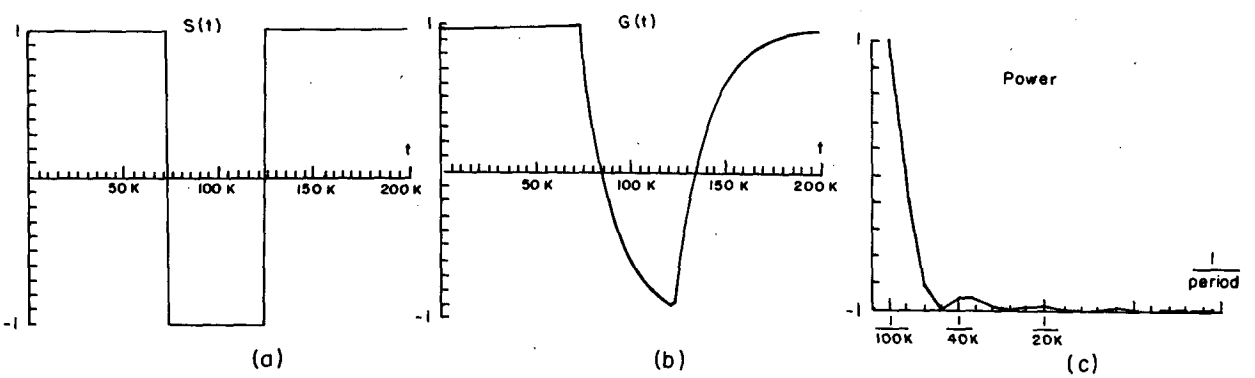

FIG. 15. As in Fig. 10 but for a threshold $T = 5.02$.

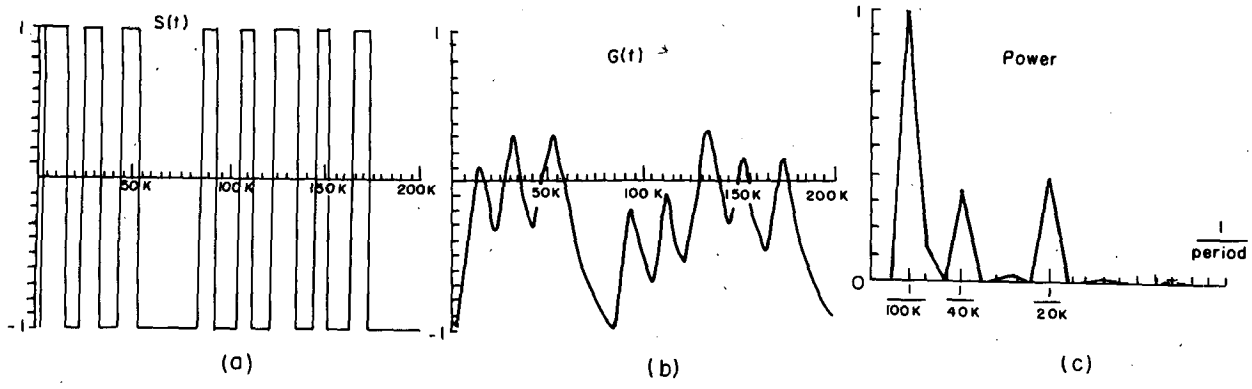

FIG. 16. As in Fig. 10 but for a threshold $T = 3.0$ and asymmetry, $\Delta = 0.6$.

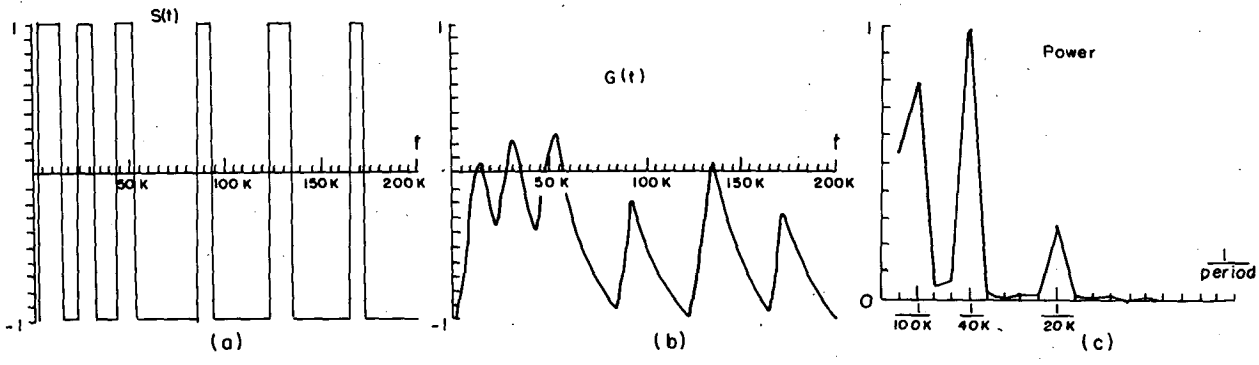

FIG. 17. As in Fig. 16 but for an asymmetry $\Delta = 0.7$.

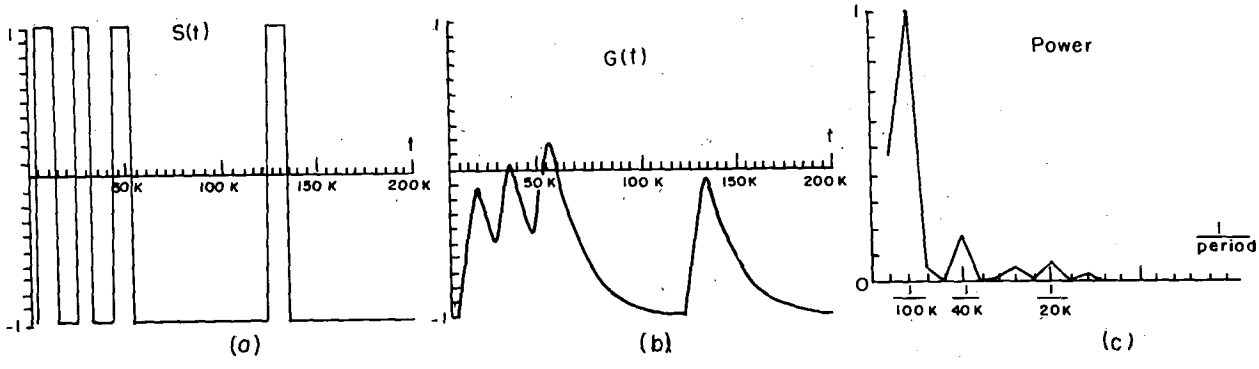

FIG. 18. As in Fig. 16 but for an asymmetry $\Delta = 0.9$.

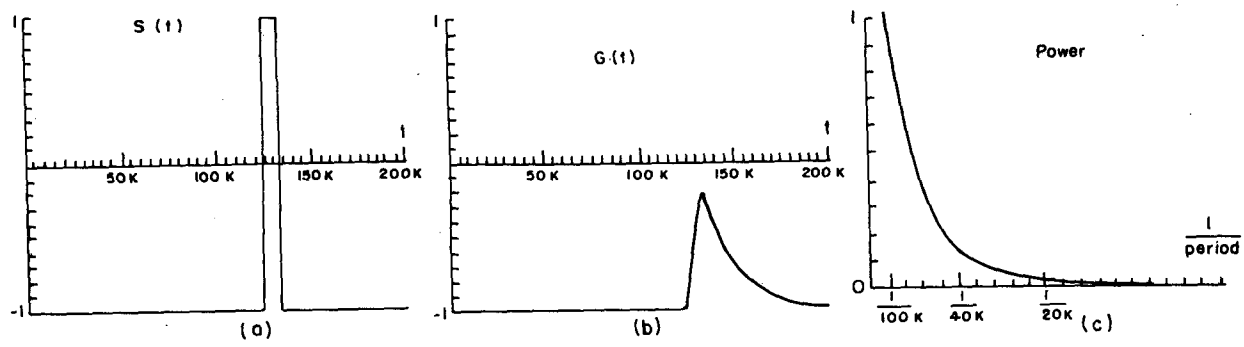

$2.1 \leq \Delta < 2.8$

FIG. 19. As in Fig. 16 but for an asymmetry $\Delta = 1.3$.

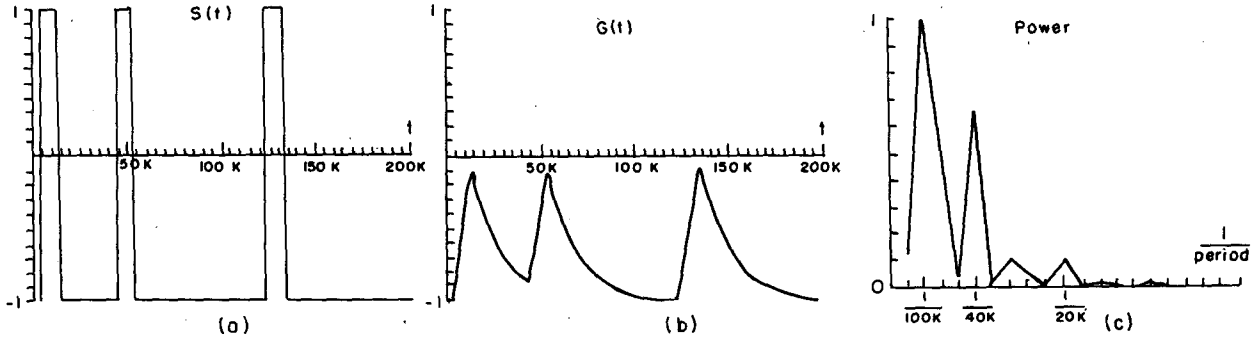

$1.3 \leq \Delta < 2.1$

FIG. 20. As in Fig. 16 but for an asymmetry $\Delta = 2.1$.

We will first look at variations in symmetric thresholds; we will then look at the effect of asymmetric thresholds.

Figures 10–15 show $S(t)$, $G(t)$ and the power spectrum of $G(t)$ for the following thresholds, -0.0, 0.0; -0.5, 0.5; -2.49, 2.49; -3.7, 3.7; -3.9, 3.9; and -5.02, 5.02. The results are, in fact, appropriate to ranges of thresholds: i.e., the results for $T = 0.0$ hold for $0.0 \leqslant T < 0.5$; $T = 0.5$ for $0.5 \leqslant T < 2.49$; $T = 2.49$ for $2.49 \leqslant T < 3.7$; $T = 3.7$ for $3.7 \leqslant T < 3.9$; $T = 3.9$ for $3.9 \leqslant T < 5.02$; and $T = 5.02$ for $5.02 \leqslant T < 5.71$. For $T \geqslant 5.71$ there is no cycling [since this exceeds the maximum excursions of $g(t)$; viz. Eq. (2)].

For $0.0 \leqslant T < 0.5$ we see that variations in $S(t)$ are strongly dominated by the 20K period as is $G(t)$, but a noticeable 100K component is already visible in $G(t)$. For $0.5 \leqslant T < 2.49$, $s(t)$ looks almost the same as for $T = 0.0$, but $G(t)$ has a significantly greater 100K component. For $2.49 \leqslant T < 3.7$ we get the results described in section 2. Note that these results obtain for a substantial range of thresholds. For the narrow range $3.7 \leqslant T < 3.9$ the glaciation actually emphasizes a 200K period while for $3.9 \leqslant T < 5.02$ the glaciation is almost completely dominated by 100K with 20K almost completely suppressed. Finally, for $5.02 \leqslant T < 5.71$ the response is again dominated by a 200K period. The main point is that virtually any threshold leads to a significant 100K response in glaciation and for $2.49 \leqslant T < 5.71$ the response is strongly dominated by either 100K or 200K periods.

Although the above results show that for $Q = Q_0$, virtually any threshold above 2.49 leads to long period dominance in glaciation, the range $2.49 \leqslant T < 3.7$ gives results that most nearly duplicate the observational results in Figs. 1 and 2. We will therefore, for this section, assume $T = 3$ is appropriate when $Q = Q_0$ + orbital variation. We next address the question of what happens when Q is subject to a slow nonorbital drift. (Recall our earlier generalized approach to Q; the posited variation could arise from variations in the solar constant and/or changing atmospheric composition.) Let us focus on the case of increasing Q. Clearly, increasing Q will eventually eliminate orbital fluctuations in glaciation (e.g., when Q + orbital variations is always greater than Q_0). Smaller increases above Q_0 will simply act to shift the thresholds. If, for example, $Q = Q_0 + \Delta$ + orbital variations, and if we assume at $Q = Q_0 +$ or-

bital variations that thresholds of -3, 3 are appropriate, then for a drift of Δ, the thresholds will change to $-3 + \Delta$, $3 + \Delta$. Having Δ between 0 and 0.5 leads to no alteration of the results at $\Delta = 0$. At $\Delta = 0.6$ one begins to see a small modification with somewhat more contribution to glaciation from the 20K period. For Δ between 0.7 and 0.8, there is a marked reduction in glaciation and the power spectrum is dominated by 40K. For Δ between 0.9 and 1.2 there is a resumed dominance of the 100K period. For Δ between 1.3 and 2 another pattern emerges that is still dominated by the 100K period. For Δ between 2.1 and 2.7 glaciation is restricted to isolated episodes occurring every 200K years, and, finally, for $\Delta \geq 2.8$ glaciation cycles cease. These results are shown in Figs. 16–20. Basically, a threshold amounting to half the maximum excursion from Q caused by orbital variations ($\Delta \geq 2.8$) will end cyclic glaciation; an increase of ⅔ of this (i.e., ⅓ of the maximum) will lead to the reduction of the glaciation cycles to isolated episodes every 200K years. There is some evidence of such behavior in Fig. 1 for times earlier than 400K BP.

4. Additional remarks

It is clear that a plausible climate model can readily selectively respond to weak 100K forcing despite stronger forcing at shorter periods. However, despite the plausibility of the model, there are clearly some arbitrary parameter choices. For a particular choice of (a_2, a_5, a_{10}) in Eq. (2) we have already examined sensitivity to threshold. However, the choice of (a_2, a_5, a_{10}) is by no means objective. Various choices have been tried with little substantive change from the present results—although the optimal threshold choices change.

One disturbing feature of the results for $G(t)$ (glaciation) is that they allow negative glaciation. In the present case this is not at all serious since the scalings of both S and G are arbitrary and negative G does not necessarily correspond to negative glaciation. The situation would change if we had an objective way of choosing $S+$ and $S-$ (as opposed to the present arbitrary choice of $+1$ and -1). Then if G turned negative the modification of (4) would be trivial: namely, it would be held at zero until S turned positive, at which point (4) would again be applicable. This offers the possibility of an additional interesting nonlinearity. However, Fig. 1 shows little evidence of protracted periods of zero glaciation.

Finally, some remark is in order on the role of CO_2 feedbacks invoked as contributors to the threshold behavior. Berner et al. (1979) note a connection between CO_2 and glaciation while we have suggested a dependence on climate state as given by sea ice/snow line position. It seems clear that, in fact, CO_2 may depend on both and that the feedback may be richer than our calculations have suggested. For example, the thresholds for S moving between $+1$ and -1 may depend on the value of G itself. Such effects remain to be explored.

Acknowledgments. This research was supported by NASA under Grant NAGW-525 and by NSF under Grant 834282-ATM.

REFERENCES

Berger, A., 1978: Long-term variations of daily insolation and quaternary climatic changes. *J. Atmos. Sci.*, **35**, 2362–2367.

Berner, W., B. Stauffer and H. Oeschger, 1979: Past atmospheric composition and climate; gas parameters measured on ice cores. *Nature*, **275**, 53–55.

Broecker, W. S., 1984: Terminations. *Milankovitch and Climate, II*, A. Berger, J. Imbrie, J. Hays, G. Kukla and B. Saltzman, Eds., Reidel, 671–686.

Budyko, M. I., 1969: The effect of solar radiation variations on the climate of the earth. *Tellus*, **21**, 611–619.

Croll, J., 1875: *Climate and Time in their Geological Relations.* Appleton, 186 pp.

Ghil, M., and H. Le Treut, 1981: A climate model with cryodynamics and geodynamics. *J. Geophys. Res.*, **86**, 5262–5270.

Held, I. M., 1976: The tropospheric lapse rate and climatic sensitivity. Ph.D. thesis, Princeton University, 217 pp.

——, and M. J. Suarez, 1974: Simple albedo feedback models of the ice caps. *Tellus*, **26**, 613–629.

Imbrie, J., and K. P. Imbrie, 1979: *Ice Ages, Solving the Mystery.* Enslow Publishers, 224 pp.

——, and J. Z. Imbrie, 1980: Modelling the climatic response to orbital variations. *Science*, **207**, 943–953.

——, J. D. Hays, D. G. Martinson, A. McIntyre, A. C. Mix, J. J. Morley, N. G. Pisias, W. L. Prell and N. J. Shackleton, 1984: The orbital theory of Pleistocene climate: Support from a revised chronology of the marine ^{18}O record. *Milankovitch and Climate, I*, A. Berger, J. Imbrie, J. Hays, G. Kukla and B. Saltzman, Eds., Reidel, 269–306.

Knox, F., and M. B. McElroy, 1984: Change in atmospheric CO_2: Influence of the marine biota at high latitude. *J. Geophys. Res.*, **89**, 4629–4637.

Lindzen, R. S., and B. Farrell, 1977: Some realistic modifications of simple climate models. *J. Atmos. Sci.*, **34**, 1487–1501.

——, and ——, 1980: The role of polar regions in global climate, and a new parameterization of global heat transport. *Mon. Wea. Rev.*, **108**, 2064–2079.

——, A. Y. Hou and B. F. Farrell, 1982: The role of convective model choice in calculating the climate impact of doubling CO_2. *J. Atmos. Sci.*, **39**, 1189–1205.

Mason, B. J., 1976: Towards the understanding and prediction of climate variation. *Quart. J. Roy. Meteor. Soc.*, **102**, 473–499.

Milankovitch, M., 1930: Mathematische Klimalehre und astronomische Theorie der Klimaschwankunger. *Handbuch der Klimatologie, I(A)*, W. Koppen and R. Geiger, Eds., Gebruder Borntraeger, 1–176.

North, G. R., 1984: The small ice cap instability in diffusive climate models. *J. Atmos. Sci.*, **41**, 3390–3395.

Peltier, W. R., and W. Hyde, 1984: A model of the ice age cycle. *Milankovitch and Climate*, A. Berger, J. Imbrie, J. Hays, G. Kukla and B. Saltzman, Eds., Reidel, 565–580.

Pollard, D., 1983: A coupled climate-ice sheed model applied to the quaternary ice ages. *J. Geophys. Res.*, **88**, 7705–7718.

Saltzman, B., A. R. Hansen and K. A. Maasch, 1984: The late quaternary glaciations as the response of a three-component feedback system to earth-orbital forcing. *J. Atmos. Sci.*, **41**, 3380–3389.

Sellers, W. D., 1969: A global climatic model based on the energy balance of the earth–atmosphere system. *J. Appl. Meteor.*, **8**, 392–400.

Suarez, M. J., and I. M. Held, 1979: The sensitivity of an energy balance climate model to variations in orbital parameters. *J. Geophys. Res.*, **84**, 4825–4836.

Weertman, J., 1976: Milankovitch solar radiation variations and ice age sheet sizes. *Nature*, **261**, 17–20.